Microvolume analysis of 226Ra by inductively coupled plasma mass spectrometry: Environmental applications to high-resolution profile of wetland soil pore waters

Marine Boudias, Anne-Laure Nivesse, Josselin Gorny, Alexandre Quémet, Nathalie Delaunay, Gilles Montavon, Catherine Landesman, Alkiviadis Gourgiotis

Microchemical Journal 204 (2024) 110971

Contents lists available at ScienceDirect

Microchemical Journal

journal homepage: www.elsevier.com/locate/microc

Microvolume analysis of ^{226}Ra by inductively coupled plasma mass spectrometry: Environmental applications to high-resolution profile of wetland soil pore waters

Marine Boudias [a,b], Anne-Laure Nivesse [c], Josselin Gorny [b], Alexandre Quémet [d], Nathalie Delaunay [a], Gilles Montavon [c], Catherine Landesman [c,*], Alkiviadis Gourgiotis [b,*]

[a] Department of Analytical, Bioanalytical Sciences, and Miniaturization, UMR 8231 Chemistry, Biology and Innovation, ESPCI Paris, PSL University, CNRS, 10 rue Vauquelin, 75005 Paris, France
[b] Institut de Radioprotection et de Sûreté Nucléaire (IRSN), PSE-ENV/SPDR/LT2S, Fontenay-aux-Roses F-92260, France
[c] Laboratoire SUBATECH, UMR 6457, CNRS-IN2P3/IMT Atlantique/Nantes Université, 4, rue Alfred Kastler, BP 20722, 44307 Nantes Cedex 3, France
[d] CEA, DES, ISEC, DMRC, Univ Montpellier, Marcoule, France

ARTICLE INFO

Keywords:
Radium
Pore waters
Diffusive equilibrium in thin-films
ICP-MS
Isotope dilution

ABSTRACT

Background: The release to the environment of natural radionuclides like ^{226}Ra due to human activities have raised concerns about human and ecosystem exposure. ^{226}Ra's resemblance to calcium and involvement in biological processes accentuate the importance of understanding its geochemical behavior and migration pathways. Soil and sediment pore waters provide valuable information but have proved to be challenging to analyze, requiring to push the limits of current sample preparation and detection methods often not scaled for low concentrated microvolumes of samples. A more efficient and accurate analytical method is therefore needed to get reliable data to support hydro-geochemical modeling.

Results: We describe here a novel comprehensive approach for accurate ^{226}Ra quantification in pore waters of a wetland located downstream of the former Rophin uranium mine. In order to highlight the migration of ^{226}Ra between the different soil layers, microvolumes of soil pore waters were *in situ* sampled up to 50 cm depth employing Diffusive Equilibrium in Thin-Films (DET) probes. The workflow included spiking DET extracts with an in-house ^{228}Ra tracer, specific solid-phase extraction with 50 mg of AnaLig Ra-01® resin, and elution fraction calcination. This process eliminated interferences and simplify the analysis matrix. Quantification relied on isotope dilution after measurement by ICP-MS hyphenated to a desolvator module and to a microsampler (150 µL injection). The resulting 1 cm-high-resolution profile revealed unusual ^{226}Ra enrichment with depth, signs of Ra mobility from the solid contamination source. These elements are essential for assessing ^{226}Ra distribution coefficients across soil horizons and subsequent wetland remobilization considerations.

Significance and novelty: This first methodological advance for ^{226}Ra constitutes a significant step to understand ^{226}Ra behavior *i.e.*, to quantify its activity level, fluxes inside of wetland soils or at the interface overlying waters/sediments. Its potential extension to studies involving other elements underscores its broader applicability in environmental research. The findings contribute to evidence-based decision-making for environmental protection and management, aiding in the preservation of ecological integrity and human health.

1. Introduction

In recent decades, anthropogenic activities such as exploitation of phosphate and uranium mines, oil and gas extraction or shale gas production by hydraulic fracturing have contributed to the release of naturally-occurring radionuclides in the environment [1]. Although their abundance is extremely low, due to their radiotoxicity, their presence in the environment may lead to chronic exposures of humans and ecosystems, the consequences of which must be assessed. Among these radionuclides, ^{226}Ra (alpha emitter, half-life: 1600 years, decay product of ^{238}U) is responsible for the formation of radon gas (^{222}Rn) and known to be radiotoxic due to its chemical similarity to Ca which is

* Corresponding authors.
E-mail addresses: catherine.landesman@subatech.in2p3.fr (C. Landesman), alkiviadis.gourgiotis@irsn.fr (A. Gourgiotis).

https://doi.org/10.1016/j.microc.2024.110971
Received 10 December 2023; Received in revised form 10 June 2024; Accepted 11 June 2024
Available online 13 June 2024

implied in many biological processes [2,3]. One of the current challenges is related to better understanding the geochemical behavior of ^{226}Ra and in particular to bring new insights on the main processes governing its migration in sediments/soils and also between the different compartments of the biosphere (*e.g.* soil to plant transfer). This implies being able to accurately quantify ^{226}Ra in accumulation zones (*e.g.* wetland soils and lake sediments located downstream from U-mines [4,5]) and in transport zones (*e.g.* pore waters). Unlike accumulation zones, quantification in transport zones currently presents many challenges: small sample volumes, high resolution vertical profiles, complex matrices, and often low ^{226}Ra concentrations.

Although several works have addressed analysis of ^{226}Ra in environmental waters reporting activities that rarely exceed 30 mBq L^{-1} [1], works on ^{226}Ra quantification in sediment or wetland soil pore waters are less abundant, probably linked to the analytical difficulties involved. In the past few decades, an important effort has been made for ^{226}Ra quantification in pore waters of marine sediments [6–9]. To this end, a few hundred of mL to few L of pore water were sampled (*e.g.* from piezometers [7]), generally passed through MnO_2 fibers for radium preconcentration, and radiometric techniques (in particular gamma spectrometry), were often used. Typical ^{226}Ra activity values were found to vary between 0.01 and 0.24 Bq/L and analytical uncertainties comprised between 1 to 15 %, based on a 1σ counting statistics [6,10]. In a more recent work, thanks to a preconcentration step and to the high sensitivity of a single-collector sector field inductively coupled plasma mass spectrometer (ICP-MS), equipped with a desolvation device and a high-sensitivity Jet interface, Yuan et al [11] determined the ^{226}Ra activity in smaller volumes of pore water (20–50 mL) from deep-sea sediments. They had achieved analytical internal precisions close to 1 % (1σ) and especially a depth resolution-profile every 5 cm. In another study, similar pore water volumes (15–30 mL) were collected in lacustrine sediments influenced by former mining sites [5]. The sediment pore waters were extracted every 5 cm with the help of Rhizons® samplers and ^{226}Ra analysis was performed by using high-efficiency, low-background, well-type germanium detectors. To achieve 1σ statistical uncertainty lower than 10 %, a counting time of 3–5 days was required. Diffusive Gradients in Thin Films (DGT) technique was also used to sample the labile ^{226}Ra fraction (fraction that is potentially dissolved in the pore water and the labile fraction bound to exchangeable soil phases) in soils [12]. This technique allowed *in situ* ^{226}Ra preconcentration in a MnO_2 based-binding gel. The analysis was performed with a sector field ICP-MS and the whole protocol allowed the achievement of a method detection limit (MDL = instrumental detection limit/preconcentration factor) as low as 0.80 mBq L^{-1} for a 24 h DGT deployment. Other DGT applications were also reported [13–15].

It is now clear that ICP-MS technology is more appropriate than radiometric techniques for accurate analysis of ^{226}Ra from small volumes of pore water [16,17]. However, even the latest advances in instrumentation, such as more specific introduction systems (desolvation devices), collision reaction cells and tandem mass spectrometry (MS/MS), rarely overcome alone spectral and non-spectral interferences [18–21]. Analysis of ^{226}Ra therefore requires the implementation of efficient sample pretreatment methods for purification and preconcentration. Among different strategies, the Solid Phase Extraction (SPE) technique is by far the most cited method for Ra [16]. Most procedures use cation exchange resins poorly selective for Ra or combinations of resins, with multi-stage and complex protocols that are not ideally suited for low sample volumes [22–24]. Three recent publications however demonstrated that AnaLig® Ra-01 resin due to its very high capacity and selectivity regarding Ra (50 mg of dry resin efficiently retain Ra from 100 mL of seawater) and compared to the aforementioned resins, offers more suitable conditions for the manipulation of small sample volumes (100 μL < V < 1 mL) with high ionic charge, thus opening up easier access to the determination of ^{226}Ra in pore waters [25–27].

In this work, we developed a new comprehensive strategy that allows to the accurate determination of a 1 cm-vertical depth profile of ^{226}Ra activity by combining the Diffusive Equilibrium in Thin-Films (DET) technique with a specific Ra extraction using the AnaLig® Ra-01 resin, and the isotopic dilution (ID)-based microsample-ICP-MS analysis. The DET technique has been developed in the 90′s by Davison and Zhang [28]. Its main application is to sample *in natura* various solutes in the sediment or soil pore-waters: major species [29], nutrients [30], products of early diagenesis processes [31–33], trace elements [30,34], etc. The solutes are equilibrated with non-bound water of hydrogel for DET technique, giving access to their total dissolved concentrations. There is therefore no removal of Ra from soil pore water, but rather an exchange reaching an equilibrium between the soil pore water and the water solution present in the hydrogel pores. Consequently, whatever the quantity of water in contact with the probe, the concentration of solutes remains constant. After deployment, the solutes are then eluted from DET hydrogel to perform chemical analysis. The elution volume depends on the analytical tool consumption, which is generally critical to the solute determination at trace or ultratrace level for DET measurements. Solute dilution is eventually compensated by the preconcentration for DGT techniques. That's probably the reason why, to the best of our knowledge, until now there is no DET applications for ^{226}Ra determination contrary to DGT measurements [12,15]. A wetland impacted by water discharges from the former Rophin uranium mine (Puy-de-Dôme, France) was selected to perform a field application. Previous investigations on this wetland highlighted significant quantities of ^{238}U and its decay products in the wetland's soil/sediment particles [35,36]. The method quantification limit (MQL) was determined, and possible routes for improvement were discussed. First interpretations that could be extracted from the drawn profile were also addressed.

2. Material and methods

2.1. Description of the site

The Rophin uranium mine is located in the northeastern Puy-de-Dôme department in France (Fig. 1). It is in close proximity to the city of Lachaux and is referenced among several mines collectively known as the Western Lachaux ore bodies. A comprehensive timeline summarizing the key events in the history of the Rophin mine and a more detailed description of the site are available in Martin *et al.* [35] and Grangeon *et al.* [37].

On a global scale, the Western Lachaux ore bodies stand out as remarkable due to the prevalence of parsonsite ($Pb_2(UO_2)(PO_4)_2{\cdot}2H_2O$) as the primary constituent of a viable deposit, as opposed to being an alteration product of pitchblende (UO_2). These ore bodies are hosted within coarse-grained peraluminous granite of the alkaline type, similar to the "Bois Noirs" granite, and are situated at the conclusion of the Variscan orogeny. These bodies primarily consist of low-temperature silica/quartz containing uranyl phosphate minerals, with parsonsite being the predominant mineral. Near the oxidized surface of the ore, one can also find autunite ($Ca(UO_2)_2(PO_4)_2.8–12\ H_2O$), tobernite ($Cu(UO_2)_2(PO_4)_2{\cdot}12H_2O$), and also pitchblende (UO_2) transported from the Bois Noirs Limouzat U mine site (Loire department, France) [38].

2.2. Reagents and materials

High purity nitric acid (HNO_3) and hydrochloric acid (HCl) were obtained by distillation (Savillex® DST-1000 system) from HNO_3 68 % Normapur (VWR Chemicals, Fontenay-sous-Bois, France) and HCl 37 % Emsure (Merck, Darmstadt, Germany). Ultrapure (UP) water was produced by a Milli-Q system (Millipore, Molsheim, France). Nitrilotriacetic acid (NTA, 99 %) was purchased from Honeywell FlukaTM (Illkirch, France), sodium nitrate Normapur (≥99.5 %) from VWR Chemicals, agarose from Bio-Rad (Marne-la-Coquette, France), and ammonia 25 % Suprapur used for pH adjustment from Merck. Two types of resins were used for chemical purification: UTEVA resin (particle size: 100–150 μm, Triskem International, Bruz, France) and AnaLig® Ra-01 resin (60–100

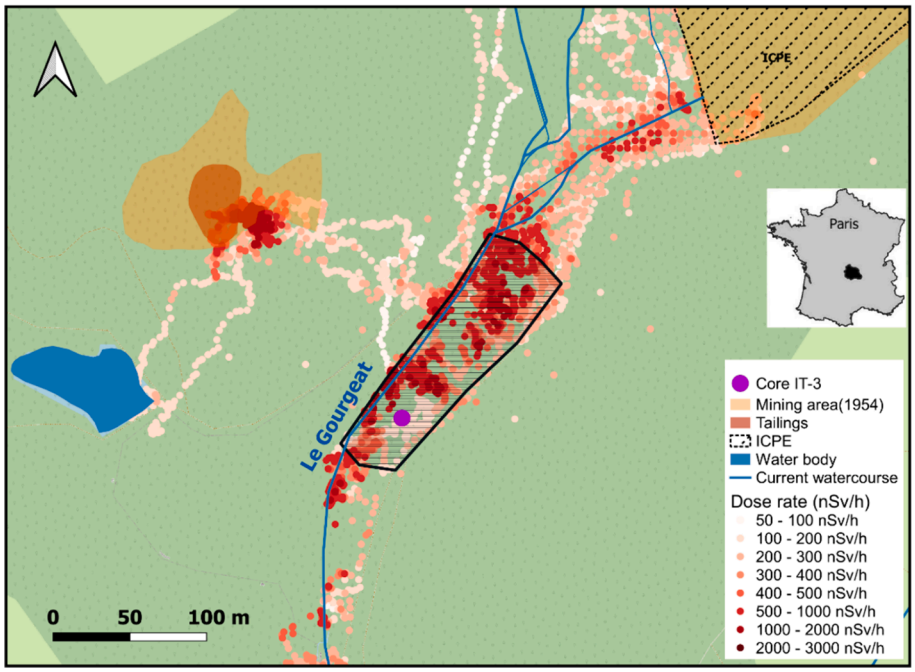

Fig. 1. Localization of the former Rophin uranium mine in France and gamma-ray dose rate mapping of the site realized in 2022. ICPE: Installations classified for environmental protection.

mesh, IBC Avanced Technologies, American fork, UT, USA). Standard plastic DET holders for sediment were provided from DGT® Research Ltd (Lancaster, England). An in-house ^{228}Ra isotope tracer was made using a mono-standard stock solution of Th (10 g L^{-1} in HNO_3 2 %, SCP Science, Villebon-sur-Yvette, France) according to the procedure described in section 2.5. A mono-elemental stock solution of U (1 g L^{-1} in 2 % HNO_3, VWR Chemicals) as well as an in-house ^{226}Ra source (activity of 11.92 ± 0.38 Bq g^{-1}, coverage factor $k = 2$) were used to optimize the ICP-MS sensitivity. U500 (atom percent: 49.696 ± 0.050 of ^{235}U and 49.711 ± 0.050 of ^{238}U, $k = 2$) [39] and IRMM-3636 (^{233}U/^{236}U: 1.01906 ± 0.00016, $k = 2$) [40] certified reference materials were used for the mass calibration of the mass spectrometer and for mass bias correction, respectively. Polypropylene tubes were used for all experiments except for calcination (see section 2.6).

2.3. DET sampling procedure and samples

DET probe consists of 75 vertically stacked slits. Slits were filled with agarose hydrogel and overlaid by a polyethersulphone filter membrane. Assembled DET samplers were immersed in 0.01 mol L^{-1} $NaNO_3$ and stored at 4 °C (in a cool box) in a tight plastic bag filled with a few drops of 0.01 mol L^{-1} $NaNO_3$ for the transport from the laboratory to the deployment site and back. The principle of a DET sampling procedure is shown in Fig. S1 in supplementary information (SI). DET probes field deployment took place in the wetland zone downstream of the former Rophin U mine (3°19′33.40″E and 46°0′8.79″N close to Core IT-3 in Fig. 1) in June 2022. The chosen sampling area was a fully saturated zone characterized by high gamma dose rates, compared to the geological background. Among the alternating layers of soil and sediment present, three layers have been identified: humus, zone inherited by the mine, and paleosol. Directly on site, DET probes were removed from their plastic bag and quickly placed in the PVC holder as described in Martin *et al.* [36]. This PVC holder integrates a set of three consecutive DET probes positions allowing a 45-cm soil profile with a duplicate configuration in back-to-back position. The PVC holder was manually driven into the soil to a 20-cm depth and fully inserted to 75 cm with the help of a mallet. During the deployment of DET probes, solutes from the adjacent medium are allowed to establish equilibrium with solutes from the agarose hydrogel, and vertical diffusion within the gel is prevented by the recessed slits separating the agarose gel-filled strips. At the end of the deployment time (24 h), probes were retrieved, wiped to remove any adhering soil particles, and rinsed with UP water. DET probes were disassembled in the laboratory and agarose slices were extracted from the plastic holders with tweezers. To obtain a 1-cm spatial resolution, five consecutive gel slices were placed in pre-weighted tubes. For each tube, the volume of gel was determined and then eluted under agitation for 24 h with 2 mL of 1 mol L^{-1} HNO_3. The eluates were then retrieved and stored at 4 °C until analysis. 1 mL were dedicated to the measurement of ^{226}Ra and the remaining 1 mL was used for other chemical analyses.

2.4. ICP-MS analysis

^{226}Ra measurements in soil pore waters were performed with an ICP-MS/MS (Agilent 8800, Agilent Technologies, Tokyo, Japan) operated in single quadrupole mode (hereafter referred as "ICP-MS") coupled to a desolvating module as introduction system (Apex Omega, ESI, Hoenheim, France). An auto-microsampler workstation (MVX-7100, Teledyne, Cetac, Omaha, Ne, USA) was used for the sample micro-volumes introduction. This autosampler offers highly consistent, syringe driven, low volume and configurable flow rate sample introduction for ICP-MS instrumentation facilitating analysis of samples with limited volumes. Sample loading was performed by an injection loop between two air gaps which allow to avoid the analyte diffusion in the carrier liquid (HNO_3 0.5 mol L^{-1}) thus preventing signal attenuation and sample cross contamination. Rates of aspiration and injection were set to ensure a good filling of the loop while avoiding bubbles. 150 μL were charged in the sample loop and injected into the plasma.

Sensitivity was daily optimized, first without the auto-microsampler, using a 1 μg L^{-1} U solution and then fine-tuned with a 10 Bq L^{-1} pure ^{226}Ra source. Optimum conditions and auto-microsampler flow settings enabled the following sensitivities to be achieved with the above solutions: 3.5 x 10^6 cps at m/z 238 (^{238}U) and 1000 cps at m/z 226, for a sample uptake close to 300 μL min^{-1}. To determine accurate isotope ratios, mass calibration and resolution were adjusted using U500 certified reference material. Mass bias was corrected by adding the reference

material IRMM-3636 (10 μL at 0.6675 ng g^{-1}) to purified samples (200 μL) prior to analysis. Operating conditions for the ICP-MS and instrument settings for the MVX-7100 are listed in Table 1. Isotopes of elements other than Ra were also monitored to ensure that the count rate was low enough not to give rise to spectral interferences, on the basis of previous interference studies carried out on Apex-HF and Apex Omega coupled to ICP-MS [26,41]. For all samples, the count rates of ^{88}Sr, ^{137}Ba, ^{146}Nd, ^{182}W, ^{208}Pb and ^{209}Bi were below 1x10^8 cps, 1x10^8 cps, 3x10^5 cps, 8x10^4 cps, 1x10^7 cps, 3x10^5 cps, respectively, which is not sufficient to induce a contribution at m/z 226. All isotope ratios were corrected for instrumental mass fractionation using the exponential law (Eq. (1)) [42,43].

$$R_A = r_A \left(\frac{m_1}{m_2}\right)^{\beta} \quad (1)$$

where R_A and r_A are the true and measured $^{226}Ra/^{228}Ra$ isotope ratios, m_1 and m_2 are the atomic masses of ^{226}Ra and ^{228}Ra (g mol^{-1}), and β is the mass bias factor. The β factor was calculated internally for each sample using the $^{233}U/^{236}U$ isotope ratio after addition of the IRMM-3636 standard to the sample. After this, it was used for mass bias correction for the $^{226}Ra/^{228}Ra$ isotope ratio.

2.5. ^{228}Ra tracer preparation

An in-house ^{228}Ra tracer was prepared by purifying 0.5 mL of 10 g L^{-1} ^{232}Th commercial standard with 2 mL of wet UTEVA resin. The detailed protocol is fully described in Table 2.

Fractions containing Ra issued from steps 4 and 5 were collected together in the same Savillex PFA Teflon vial, evaporated to dryness using an EvapoClean system (Analab) (90 °C overnight), and re-solubilized in 0.5 mol L^{-1} HNO_3 (2 mL). No ^{232}Th was detected in the Ra elution fraction collected (decontamination factor for Th was found to be 99.9 %), meaning the purification was efficient. Afterwards, two aliquots of 0.1 mL were taken from the Ra elution fraction and used to characterize the tracer before its use to estimate (i) the $^{228}Ra/^{226}Ra$ isotope ratio (^{226}Ra impurities result from the decay of ^{230}Th) and (ii) the ^{228}Ra concentration by ID.

For ID, the aliquot was spiked with a well characterized ^{226}Ra solution prepared from an in-house ^{226}Ra source at 11.92 ± 0.38 Bq g^{-1}. After spiking and adjusting the molarity of the sample to 0.5 mol L^{-1} HNO_3, 24 h isotopic equilibration was waited. IRMM-3636 isotopic reference material was added (40 μL at 0.002 ng g^{-1} of ^{236}U) to each aliquot, spiked and unspiked, before analysis with Apex Omega-ICP-MS (see instrument settings in Table S1), to correct for the instrumental mass fractionation.

Table 1
ICP-MS acquisition parameters for the measurement of ^{226}Ra in pore waters.

Auto-microsampler MVX-7100 (Teledyne, Cetac)	
Injected sample volume (μL) / Filling rate of the injection loop (μL min^{-1})	150 / 300
Volume of HNO_3 (carrier) (μL) / Injection rate (μL min^{-1})	1200 / 125
	Apex Omega
Spray chamber temperature	140 °C
Peltier Cooler temperature	3 °C
Desolvator temperature	155 °C
N_2 gas (desolvating system)	3 L min^{-1}
Ar gas (desolvating system)	4 L min^{-1}
Agilent 8800 ICP-MS	
Stabilization time (s)	95
Isotopes monitored	^{226}Ra, ^{228}Ra, ^{88}Sr, ^{137}Ba, ^{146}Nd, ^{182}W, ^{208}Pb, ^{209}Bi, ^{233}U, ^{236}U
Peak pattern	1 point
Integration time (s)	2 for m/z 226 and 228; 0.1 for all other m/z
Number of replicates	25
Number of sweeps	100

Table 2
Protocol for preparation of the in-house ^{228}Ra tracer.

Step	Procedure	Solution (volume)
1	Column washing	0.1 mol L^{-1} HCl (6 mL)
2	Column washing	UP water (6 mL)
3	Conditioning	3 mol L^{-1} HNO_3 (6 mL)
4	Sample loading	Sample in 3 mol L^{-1} HNO_3 (~0.5 mL)
5	Ra elution	3 mol L^{-1} HNO_3 (6 mL)
6	Fractions issued from steps 4 and 5 gathered and evaporated to dryness at 90 °C	
7	Recovering in 0.5 mol L^{-1} HNO_3 (2 mL)	

The ID equation (Eq. (2)) allowed to calculate the ^{228}Ra concentration. ^{228}Ra being not brought by the ^{226}Ra spike, Eq. (2) is a simplified form of the general ID equation. In Eq. (2) uncertainties were propagated using a Monte-Carlo simulation approach. From the above methodology, an isotope ratio $^{228}Ra/^{226}Ra$ of 2.857 ± 0.082 ($k = 2$) and a ^{228}Ra concentration of 0.433 ± 0.016 pg g^{-1} ($k = 2$) were determined. The value of the $^{228}Ra/^{226}Ra$ ratio was determined again later in that study by HR-ICP-MS (Element XR, Thermo Fisher Scientific) which offers improved sensitivity due to a higher voltage applied to the extraction lenses and a better vacuum at the interface, thereby achieving greater accuracy. The new value was found to be 2.844 ± 0.013 ($k = 2$) (at the date of ^{232}Th separation) and all ^{226}Ra concentrations in this study were calculated according to this value. The value determined by ICP-MS is in agreement with that measured by HR-ICP-MS. It is worth mentioning that for all calculations, the tracer's radioactive decay was taken into account since its purification/characterization date and until the day of analysis.

$$\left[^{228}Ra\right]_s = \frac{\left[^{226}Ra\right]_{sp}}{(R_m - R_s)} \times \frac{M_{sp}}{M_s} \times \frac{228}{226} \quad (2)$$

where $[^{228}Ra]_s$ and $[^{226}Ra]_{sp}$ are the ^{228}Ra and ^{226}Ra concentrations of the sample (aliquot unspiked) and of the spike solution (pg g^{-1}), respectively, M_s and M_{sp} are the mass of sample and spike solutions mixed together (g), 226 and 228 are the atomic mass of the corresponding isotopes (g mol^{-1}), and R_s and R_m are the $^{226}Ra/^{228}Ra$ measured isotope ratios in the unspiked sample (*i.e.* unspiked aliquot) and in the mixture (*i.e.* spiked aliquot).

2.6. Radium extraction

For all samples, namely 45 DET extracts (1 mL) and 1 procedural blank (DET matrix, extraction on AnaLig, calcination, resuspension), the extraction of ^{226}Ra was performed with AnaLig® Ra-01 resin, using a procedure close to that developed in a previous paper in which this resin was thoroughly characterized (*i.e.* affinity with a wide range of elements in different acid media, elution profiles and spectral interferences) [26]. To quantify ^{226}Ra by ID, samples were previously weighed up to about 1 g before adding 50 μL of ^{228}Ra tracer. It should be noted that due to its short half-life (5.75 years) and to the low ^{232}Th concentrations in the sediments and soils of the wetland (variations between 6 and 30 mg kg^{-1}), the concentration of naturally occurring ^{228}Ra in pore waters is negligible. 50 mg of resin were introduced into 1 mL pipette tip between two polytetrafluoroethylene frits and extractions were performed using a Manifold. As shown in Table 3, the resin was first washed with UP water (3 mL), 6 mol L^{-1} HCl (3 mL) and again with UP water (3 mL) before being conditioned with 1 mol L^{-1} HNO_3 (5 mL). After 24 h isotope equilibration, the 1 mL of sample in HNO_3 1 mol L^{-1} was loaded on the resin which was then washed with 0.1 mol L^{-1} HCl (5 mL) and 6 mol L^{-1} HCl (5 mL) to remove Sr, Cs, Ba (partially), Tl, and Pb before increasing the pH with a small volume of UP water (200 μL) and finally eluting Ra with 0.12 mol L^{-1} NTA at pH 10 (0.5 mL). The elution fraction collected in an acid-washed borosilicate tube was evaporated to dryness using an

Table 3
Protocols for the chemical purification of Ra from DET extracts.

Step	Procedure	Solution (volume)
1	Column washing	H_2O (3 mL), 6 mol L^{-1} HCl (3 mL), H_2O (3 mL)
2	Conditioning	1 mol L^{-1} HNO_3 (5 mL)
3	Sample loading	Sample in 1 mol L^{-1} HNO_3* (~1 mL)
4	Matrix elution	0.1 mol L^{-1} HCl (5 mL)
5	Matrix elution	6 mol L^{-1} HCl (5 mL)
6	pH increase	200 µL of UP water
7	Ra elution	0.12 mol L^{-1} NTA pH 10 (0.5 mL) (collection in a borosilicate tube)
8	Evaporation to dryness at 90 °C	
9	Calcination at 450 °C (~1 night)	
10	Recovering in 0.5 mol L^{-1} HNO_3 (200 µL)	

* In Verlinde et al. [26], the conditioning and loading steps were performed in 0.1 mol L^{-1} HCl to ensure strong Ra retention and low Sr retention. However, since the distribution coefficients were not significantly different in 1 mol L^{-1} HNO_3 compared to 0.1 mol L^{-1} HCl, and the gel strips were eluted with 1 mol L^{-1} HNO_3, the procedure was modified to avoid the need for an evaporation step.

EvapoClean system (Analab) at 90 °C before decomposing NTA (melting point: 242 °C [44]) at 450 °C in a muffle furnace overnight. Indeed, experience showed that presence of NTA in the analyzed fraction was responsible for matrix effects, fouling, and sometimes clogging of the ICP-MS introduction system leading thus to significant reduction of the detected signal (see Figure S2 in SI). This procedure improvement allows now to easily analyze more than 50 samples during an analytical session. The next day, Ra was recovered in 0.5 mol L^{-1} HNO_3 (0.5 mL) by heating the closed glass bottle using an EvapoClean system at 90 °C for 1–2 h to help its re-solubilization. The supernatant was finally evaporated to reduce its volume to 200 µL (preconcentration factor of 5) for ICP-MS analysis. It should be emphasized that purification on AnaLig® Ra-01 resin also contributes to eliminate residual ^{228}Th produced by the radioactive decay of ^{228}Ra.

2.7. ^{226}Ra determination

2.7.1. Spiking optimization

ID requires optimal spiking to obtain the best accuracy (*i.e.* the minimum relative uncertainty of the ^{226}Ra concentration in the sample, $[^{226}Ra]_s$). The uncertainty of the R_{SP} and R_m ratios (*i.e.* ^{226}Ra/^{228}Ra isotope ratios of the spike and of the mixture) is propagated with the aim of finding an R_m that gives the minimum relative uncertainty on $[^{226}Ra]_s$. This leads to Eq. (3) describing the error multiplication factor (F) as a function of R_m [45]. The F factor corresponds to the multiplication factor of the uncertainty degradation. The most accurate conditions for the ID are obtained when the F factor is equal to 1.

$$F = \frac{1/R_{sp}}{(1/R_{sp} - 1/R_m)} \tag{3}$$

The F factor as a function of R_m is shown in Fig. 2 for different spike enrichments and for a sample containing 100 % of ^{226}Ra. For the spike enrichment used in this study (*i.e.* 74 %), the F factor tends to 1 (*i.e.* the best ID condition) as R_m gets closer to R_S (*i.e.* ^{226}Ra/^{228}Ra isotope ratio of the sample) and becomes larger as R_m approaches R_{sp} (*i.e.* the $[^{226}Ra]_s$ relative uncertainty is deteriorated). The best choice would appear to be $R_m = R_S$ (*i.e.* when no spike is used), but this makes no sense for an ID measurement. A compromise must be found between minimum F factor (*e.g.* F factor < 2) and spike addition (*e.g.* $[Ra]_{sp}/[Ra]_s$ ratio in the mixture greater than 0.1). Acceptable conditions can be determined graphically: measuring R_m between 0.7 and 14 appears to provide an interesting compromise between a low F factor and the need to add a spike. The use of a highly enriched spike is interesting to make the ID implementation easier. The F factor curve shifts increasingly to the left as the spike is enriched. The area where the F factor is minimal is larger

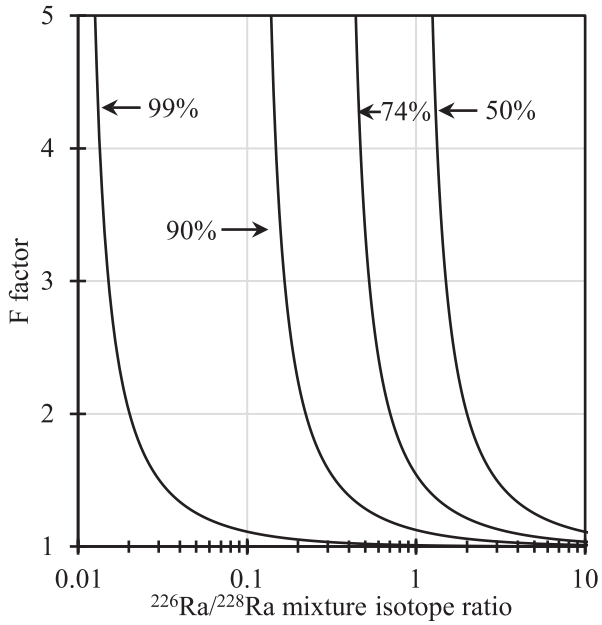

Fig. 2. Error multiplication factor F as a function of the ^{226}Ra/^{228}Ra mixture isotope ratio for ^{228}Ra isotope enrichment of 50 % (R_{sp} = ^{226}Ra/^{228}Ra = 1), 74 % (corresponding to the spike used in this study, R_{sp} = 0.35), 90 % (R_{sp} = 0.11) and 99 % (R_{sp} = 0.01) of the spike.

for highly enriched spikes than for low-enriched spikes, which favors the ID implementation and the access to the lowest uncertainty. For example, for an enrichment of the spike of 99 % (Fig. 2), measuring R_m between 0.02 and 10 appears to provide an interesting compromise: the isotope ratios range is higher than for the spike used in this study (R_m between 0.7 and 14). It is worth noting that using a spike with a higher enrichment than the one used in this study will not have a significant effect on the detection limit (see dedicated section in SI).

2.7.2. Concentration calculation

The concentration of ^{226}Ra in the purified sample was determined by ID according to Eq. (4). The associated uncertainty was estimated by combining the uncertainties from each term of Eq (4) and is available in SI (Eq. (S4)).

$$[^{226}Ra]_s = [^{228}Ra]_{sp}(R_m - R_{sp})\frac{m_{sp}}{m_s}\frac{226}{228} \tag{4}$$

where $[^{226}Ra]_s$ and $[^{228}Ra]_{sp}$ are the concentrations of ^{226}Ra and ^{228}Ra, in the sample and the spike solution, respectively in (pg g^{-1}), m_s and m_{sp} are the mass of sample and spike solutions mixed together (g), 226 and 228 are the atomic mass of the corresponding isotopes (g mol^{-1}), and R_{sp} and R_m are the ^{226}Ra/^{228}Ra isotope ratios of the tracer and in the mixture solution respectively.

Finally, the ^{226}Ra concentrations in DET gel strips (c_{DET}), *i.e.* those in the pore waters collected at different depth levels, were determined from Eq. (5). It should be noted that we considered density of pore waters equal to 1.

$$c_{DET} = [^{226}Ra]_s \times \frac{V_{eluent} + V_{gel}}{V_{gel}} \tag{5}$$

Where $[^{226}Ra]_s$ is the ^{226}Ra concentration determined by ID after its purification (pg mL^{-1}) and V_{eluent} and V_{gel} are the volumes of eluent and of the agarose gel slices (mL), respectively.

^{226}Ra concentrations were converted in activities (Bq/L) by using the next equivalence: 1 pg mL^{-1} = 36.6 Bq/L. All the calculations were implemented in an Excel file available in the SI.

2.8. Estimation of the method quantification limit

To estimate the MQL, five strips of agarose hydrogel (representing a volume of about 25 µL × 5 = 125 µL) were placed in 3 mL of a 10 mmol L^{-1} $NaNO_3$ solution (pH 5.5 ± 0.1) containing varying ^{226}Ra activities (0.02; 0.05; 0.1; 0.5; 1; 5; 10 Bq L^{-1}). The lowest activity selected for this test (0.02 Bq L^{-1}) actually corresponds to the instrumental LOQ estimated from the analysis of a 0.5 mol L^{-1} HNO_3 blank solution in Apex-ICP-MS [26]. The immersion solution in which agarose hydrogel strips could freely float was stirred for 24 h using a Bioblock scientific 74,402 orbital shaker (200 rpm). After 24 h of immersion time, each group of 5 gel strips were collected with a polypropylene tweezer in a polyethylene tube and weighted. After a complete gel strips dissolution in contact with 100 µL of 3 mol L^{-1} HNO_3, ^{226}Ra determination was performed according to the procedure presented in Fig. 3(a).

3. Results and discussion

To accurately determine a 1 cm-vertical depth profile of ^{226}Ra activities in pore waters sampled from a wetland located near a former French mining site, DET probes were deployed and the corresponding DET extracts purified before being injected in ICP-MS.

3.1. Selection of the data evaluation method

The injection of microvolumes into the ICP-MS (150 µL) generates isotope transient signals. Therefore, in addition to sample collection, purification and analysis steps, data evaluation is critical to determine accurate isotope ratios resulting from transient signals. The sample signal time window is directly related to the sample volume and to its injection rate (Fig. 4).

To determine the $^{226}Ra/^{228}Ra$ isotope ratio of the sample-tracer mixture (R_m) which is needed for the ^{226}Ra concentration calculation (Eq. (4), the Linear Regression Slope (LRS) approach was used [46,47]. The LRS is a proven method for assessing isotope ratios from transient signals. Isotope ratios are calculated from the linear regression slope of the respective isotope signals (including the signal background). The blank-free isotope ratio $^{226}Ra/^{228}Ra$ is given by the slope of the linear regression and the intercept corresponds to the ^{226}Ra blank (instrumental) in the sample. Note that typical intercept values remain insignificant compared to the ^{226}Ra signal, as shown in Fig. 4b.

3.2. Method quantification limit

By using the intercept values presented in Fig. 4, it is possible to obtain the blank for each individual sample and proceed to the calculation of the Limit Of Quantification (LOQ). A total of 44 intercepts were used (45 samples with one outlier excluded), yielding an average value for the ^{226}Ra blank of 0.57 cps with a standard deviation of 0.59 (1 sigma) (see also Supporting Information, Figure S4). Based on the instrumental sensitivity at 300 µL min^{-1}, it is possible to estimate the sensitivity at a flow rate of 125 µL min^{-1} which corresponds to the sample injection flow rate assuming a linear function between flow rate and sensitivity. Consequently, for an instrumental sensitivity of 42 cps / (Bq L^{-1}) and using the average and standard deviation (std) of the blank mentioned above, a LOQ of ~ 0.15 Bq L^{-1} is obtained (LOQ=(blank average + 10 x std)/instrumental sensitivity). This value is close to the experimental LOQ of 0.1 Bq L^{-1} found in Fig. 5. However, the difference between the two LOQ values could be explained by the estimated sensitivity at 125 µL min^{-1} (there may not be a purely linear function between flow rate and sensitivity) and/or a more robust blank calculation (44 intercepts *versus* one procedural blank during the lab experiment, as shown in Fig. 3a). It is worth noting that in this experiment (called "*Lab Exp.*" in Fig. 3(a)), agarose hydrogel strips were dissolved and the entire volume of solution (around 275 µL) was purified by SPE, thus the measured ^{226}Ra activities directly correspond to those in the gel strips. In experiment involving real pore waters (called "*Field Exp.*" in Fig. 3(b)), agarose hydrogel strips were first eluted with 2 mL of eluent and only 1 mL of the total volume were then purified by SPE. Hence, based on the experimental LOQ of 0.1 Bq L^{-1} aforementioned for the "*Lab Exp.*" and taking into account dilution factors of both protocols, the MQL for the "*Field Exp.*" should be 0.21 Bq L^{-1}. By using the LOQ calculated by averaging the intercepts of 44 samples, the MQL was found to be close to 0.32 Bq L^{-1}. The final MQL was estimated by averaging these two values and was found to be 0.27 Bq L^{-1}.

It should also be noted that our procedural blank mentioned in

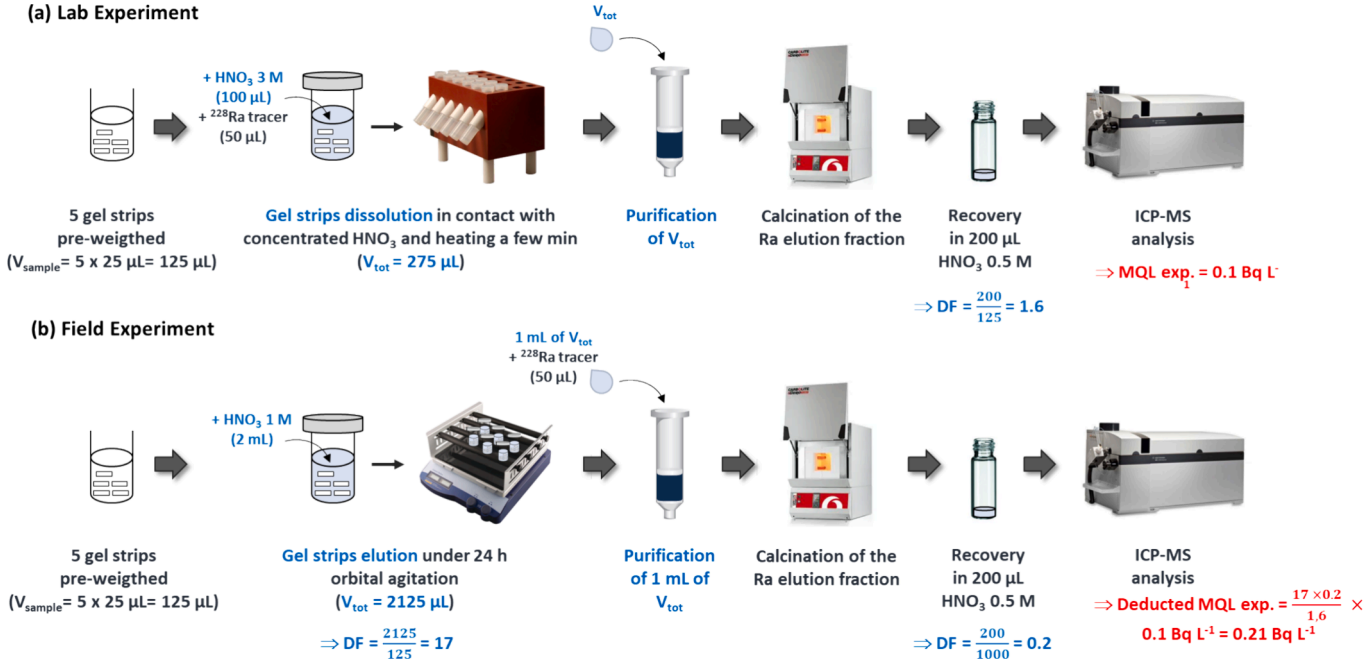

Fig. 3. Workflows of (a) the Lab Experiment implemented to evaluate the MQL from simulated pore waters containing ^{226}Ra and of (b) the Field Experiment involving real pore waters.

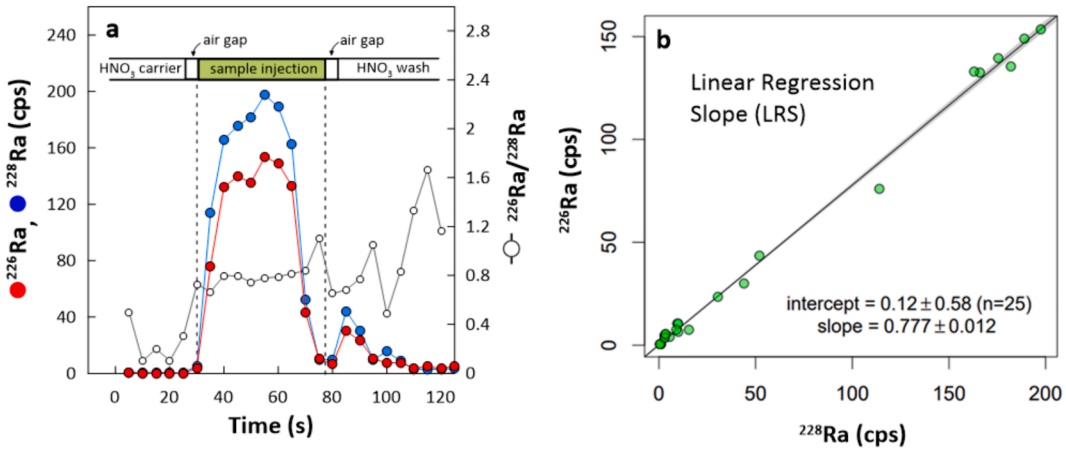

Fig. 4. Transient isotope signals for ^{226}Ra and ^{228}Ra (a) and application of the Linear Regression Slope method for the calculation of the ^{226}Ra/^{228}Ra isotope ratio (b).

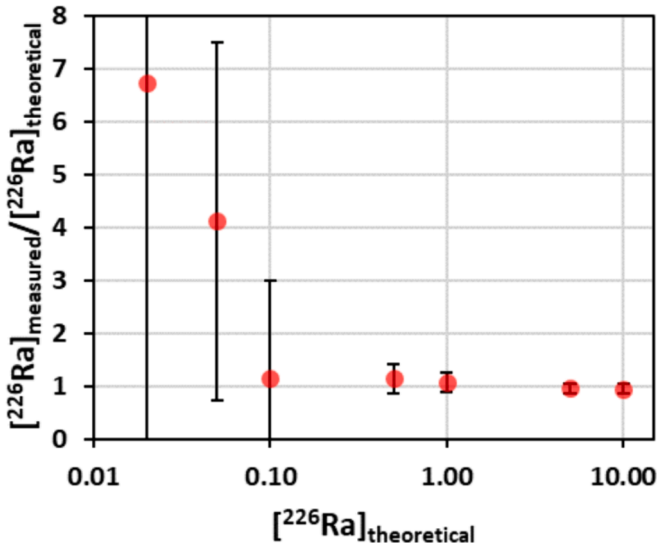

Fig. 5. Ratios between measured and theoretical ^{226}Ra activities as a function of theoretical ^{226}Ra activities for the different agarose strips in contact with standards in 10 mmol L^{-1} $NaNO_3$. Error bars correspond to an uncertainty of 2 sigma.

section 2.6. also underwent a calcination step in borosilicate glass and showed no signal at *m/z* 226 other than that brought by the spike (the accurate ^{226}Ra/^{228}Ra ratio of the spike was measured, confirming that there were no significant interferences at *m/z* 226 and 228).

3.3. *Pore water profile of ^{226}Ra in a former uranium mine*

The deployment of DET probes in the wetland downstream of the former Rophin U mine has allowed to obtain a centimetric-depth profile of ^{226}Ra activity over 45 cm (Fig. 6). This profile crosses the three characteristic layers of the wetland, the humus layer (0 to −13 cm with ^{226}Ra activities of a few thousand Bq kg^{-1}), the area inherited by the mine or source term (−13 to –32 cm with high ^{226}Ra activities of several tens of thousands of Bq kg^{-1}) and the paleosol (–32 to −50 cm with a geochemical background in ^{226}Ra of a few hundred Bq kg^{-1}). This division may vary according to the core sampling zone in the wetland. As values exceeded the MQL (0.27 Bq L^{-1}, the red line in Fig. 6), we clearly demonstrate the feasibility to perform DET application for ^{226}Ra. ^{226}Ra activities were relatively constant up to 29 cm of depth with a value of 1.6 Bq L^{-1} (RSD: 28 %) before progressively increasing up to 8.6 ± 1.2 Bq L^{-1} (k = 2). These activity level largely exceeded typical values of ^{226}Ra in environmental waters (often < 30 mBq L^{-1} in seawater, rivers, lakes, and groundwater) [1], probably linked to past inputs of mining materials enriched in ^{226}Ra (particles of U ores) sequestered in humus and inherited zone layers [35–37]. In addition, the paleosol is the zone where the ^{226}Ra contents are highest in the pore water but, as previously stated, where the ^{226}Ra contents are lowest in the soil which does not justify these values. This result would therefore indicate either (i) a downward migration of ^{226}Ra which is probably due to the movement of the water table that rises and leaches the area inherited from the mine and contaminated with ^{226}Ra, thus mobilizing ^{226}Ra or (ii) a K_d much lower in the paleosol region. One other important piece of information extractable from these measurements and ^{226}Ra activities in the solid phase is the radium distribution coefficient (K_d) in the soil/sediment core, which is a key element for assessing the remobilization of this nuclide in the Rophin wetland. This high ^{226}Ra resolution-profile will allow an accurate K_d determination for the different soil layers opening new possibilities for accurate ^{226}Ra geochemical behavior modeling thus highlighting the importance of the data collected. This topic will be addressed in a future work.

4. Conclusion

The purpose of this study was to develop a reliable strategy to allow ^{226}Ra concentrations determination in soil or sediment pore waters, which constitute valuable data for understanding the behavior of this radionuclide in environment. The use of AnaLig® Ra-01 combined with the use of an autosampler dedicated to micro-volumes allowed to obtain a 1 cm-resolution-profile of ^{226}Ra in pore waters collected with DET probes on the wetland located downstream of a former French mining site, and this from very small sample volumes with complex matrices (125 μL).

From an analytical perspective, the results uncertainties could be further enhanced by means of a purer ^{228}Ra tracer (less ^{226}Ra impurities). In that sense, investment of laboratories making certified standards in the production of a ^{226}Ra/^{228}Ra source would be truly beneficial. It is worth mentioning that to achieve an accurate ^{226}Ra concentration using the ID method, the accurate measurement of ^{226}Ra/^{228}Ra isotope ratio is crucial, as this parameter carries the greatest uncertainty.

Such methodology could also be applied to isotope studies targeting other elements, such as Pb or U. Alternatively, the combined use of DET − DGT probes could enable to qualify the availability and mobility degree of ^{226}Ra. From a geochemical point of view, to go even further in data interpretation, it will be necessary to combine data in pore waters and in solids for the different horizons, which will allow to define

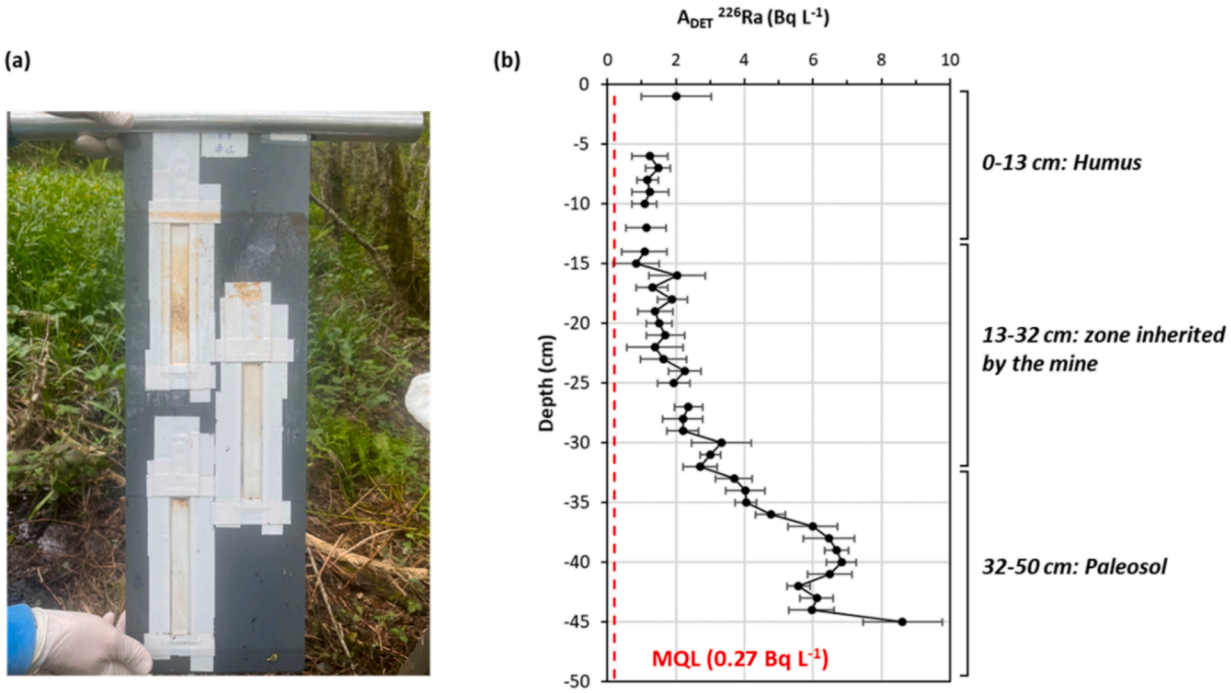

Fig. 6. Pore water profile of ^{226}Ra at Rophin site. Pore waters were sampled using DET in a soil composed of three layers. Error bars correspond to expanded uncertainties with a coverage factor $k = 2$.

partition coefficient (K_d) values, one of the input parameters necessary to establish a transport model of ^{226}Ra in this wetland. Finally, performing other sampling campaigns at different seasons over several years would bring information on factors governing ^{226}Ra mobility at larger scale.

5. Perspectives

In this section are listed some key actions that can improve the method performances in terms of spatial resolution, limits of quantification and method accuracy.

- Deploying several DETs side by side and combining the gel strips corresponding to the same level at the time of elution could be considered to further decrease the profile resolution, which is currently of 1 cm, while keeping a sufficient sample volume and amount of ^{226}Ra for the sample processing and analysis steps. This is acceptable subject to the absence of lateral heterogeneities in the considered deployment area.
- According to Verlinde *et al.* [26], a gain of a factor of 10 in terms of quantification limit was observed between the ICP-MS/MS Agilent 8800 and the sector field HR-ICP-MS Element. Therefore, the use of a sector field ICP-MS instrument with the APEX Omega desolvator as the introduction system and the microsampler can offer a significant improvement of the quantification limit of the previously developed methodology. Vieira *et al.* also demonstrated impressive performance for Ra isotope analysis, using a flat-top kit and HR-ICP-MS, which could be explored and compared in future work [23].
- Finally, the use of a high purity tracer (low presence of ^{226}Ra) can give more spiking "flexibility" for achieving a low *F* factor. In fact, according to Fig. 2, for high purity spikes, a higher range of the ^{226}Ra/^{228}Ra mixing ratio can be tolerated by the ID equation ensuring a low *F* factor and thus an improvement of the method accuracy. This point can play a key role in samples with completely unknown ^{226}Ra concentrations.

To obtain high purity spikes it is mandatory to dispose thorium solutions with low ^{230}Th/^{232}Th ratios: the lower the ^{230}Th/^{232}Th, the higher the ^{228}Ra/^{226}Ra ratio, as can be seen in Fig. 7. Therefore, another action that can improve ^{228}Ra purity for a given old thorium solution, is a chemical separation of thorium from radium to obtain a pure thorium solution which will re-generate radium with a higher purity. According to Fig. 7, the first years of thorium decay, ^{228}Ra/^{226}Ra ratio remains significantly higher compared with that of an older solution. Moreover, for highly concentrated ^{232}Th solutions, sufficient ^{228}Ra concentrations can be produced in 2–3 years after the chemical separation, thus allowing the fabrication of a higher purity ^{228}Ra spike (according to the procedure described in section 2.5).

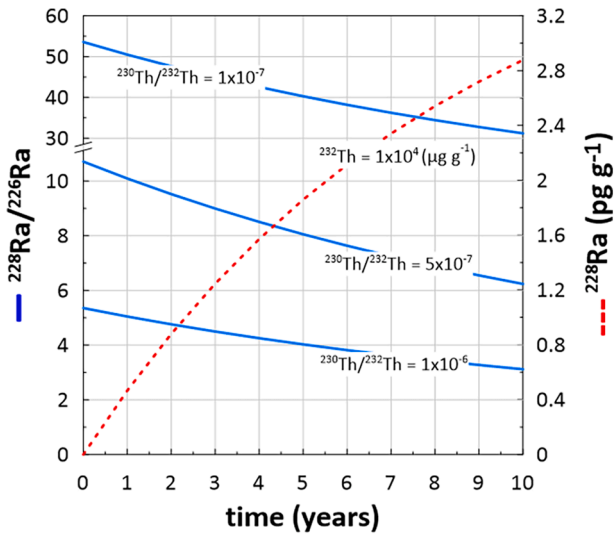

Fig. 7. ^{228}Ra concentration and ^{228}Ra/^{226}Ra isotope ratios, evolution as function of time, of pure thorium solutions (without radium at t = 0 y) with [^{232}Th] = 10 g L^{-1} and with different ^{230}Th/^{232}Th isotope ratios.

CRediT authorship contribution statement

Marine Boudias: Writing – review & editing, Writing – original draft, Validation, Investigation, Conceptualization. **Anne-Laure Nivesse:** Writing – review & editing, Resources, Investigation. **Josselin Gorny:** Writing – review & editing, Investigation. **Alexandre Quémet:** Writing – review & editing, Software. **Nathalie Delaunay:** Writing – review & editing. **Gilles Montavon:** Writing – review & editing. **Catherine Landesman:** Writing – review & editing, Resources, Investigation. **Alkiviadis Gourgiotis:** Writing – review & editing, Writing – original draft, Supervision, Resources, Project administration, Funding acquisition, Conceptualization.

Declaration of competing interest

The authors declare that they have no known competing financial interests or personal relationships that could have appeared to influence the work reported in this paper.

Data availability

Data will be made available on request.

Acknowledgements

This is PATERSON, the IRSN's mass spectrometry platform, contribution n°23.

The authors are grateful to the ZATU Pilot Workshop within the Hercynian orogeny (ZATU, https://zatu.org/).

Appendix A. Supplementary data

Supplementary data to this article can be found online at https://doi.org/10.1016/j.microc.2024.110971.

References

[1] I.A.E. Agency, The Environmental Behaviour of Radium, Revised Edition,, International Atomic Energy Agency, 2014.
[2] D. Brugge, V. Buchner, Radium in the environment: exposure pathways and health effects, 27 (2012) 1–17. https://doi.org/10.1515/reveh-2012-0001.
[3] M.C. Thorne, J. Vennart, The toxicity of 90Sr, 226Ra and 239Pu, Nature 263 (1976) 555–558, https://doi.org/10.1038/263555a0.
[4] A. Mangeret, P. Blanchart, G. Alcalde, X. Amet, C. Cazala, M.-O. Gallerand, An evidence of chemically and physically mediated migration of 238U and its daughter isotopes in the vicinity of a former uranium mine, J. Environ. Radioact. 195 (2018) 67–71, https://doi.org/10.1016/j.jenvrad.2018.08.018.
[5] A. Mangeret, J.-L. Reyss, M. Seder-Colomina, L. Stetten, G. Morin, A. Thouvenot, M. Souhaut, P. van Beek, Early diagenesis of radium 226 and radium 228 in lacustrine sediments influenced by former mining sites, J. Environ. Radioact. 222 (2020) 106324, https://doi.org/10.1016/j.jenvrad.2020.106324.
[6] J.K. Cochran, S. Krishnaswami, Radium, thorium, uranium, and 210 Pb in deep-sea sediments and sediment pore waters from the North Equatorial Pacific, Am. J. Sci. 280 (1980) 849–889, https://doi.org/10.2475/ajs.280.9.849.
[7] A.L.H. Hughes, A.M. Wilson, W.S. Moore, Groundwater transport and radium variability in coastal porewaters, Estuar. Coast. Shelf Sci. 164 (2015) 94–104, https://doi.org/10.1016/j.ecss.2015.06.005.
[8] V. Rodellas, J. Garcia-Orellana, G. Trezzi, P. Masqué, T.C. Stieglitz, H. Bokuniewicz, J.K. Cochran, E. Berdalet, Using the radium quartet to quantify submarine groundwater discharge and porewater exchange, Geochim. Cosmochim. Acta 196 (2017) 58–73, https://doi.org/10.1016/j.gca.2016.09.016.
[9] A. Alorda-Kleinglass, J. Garcia-Orellana, V. Rodellas, M. Cerdà-Domènech, A. Tovar-Sánchez, M. Diego-Feliu, G. Trezzi, D. Sánchez-Quilez, A. Sanchez-Vidal, M. Canals, Remobilization of dissolved metals from a coastal mine tailing deposit driven by groundwater discharge and porewater exchange, Sci. Total Environ. 688 (2019) 1359–1372, https://doi.org/10.1016/j.scitotenv.2019.06.224.
[10] D. Kadko, J. Kirk Cochran, M. Lyle, The effect of bioturbation and adsorption gradients on solid and dissolved radium profiles in sediments from the eastern equatorial Pacific, Geochim. Cosmochim. Acta 51 (1987) 1613–1623, https://doi.org/10.1016/0016-7037(87)90342-5.
[11] L. Yuan, P. Cai, X. Jiang, W. Geibert, Y. Cheng, Y. Chen, Precise measurement of 226Ra/230Th disequilibria in deep-sea sediments by high-sensitivity ICP-MS, Chem. Geol. 620 (2023) 121351, https://doi.org/10.1016/j.chemgeo.2023.121351.
[12] M. Leermakers, Y. Gao, J. Navez, A. Poffijn, K. Croes, W. Baeyens, Radium analysis by sector field ICP-MS in combination with the Diffusive Gradients in Thin Films (DGT) technique, J. Anal. at. Spectrom. 24 (2009) 1115–1117, https://doi.org/10.1039/B821472G.
[13] Y. Gao, W. Baeyens, S. De Galan, A. Poffijn, M. Leermakers, Mobility of radium and trace metals in sediments of the Winterbeek: Application of sequential extraction and DGT techniques, Environ. Pollut. 158 (2010) 2439–2445, https://doi.org/10.1016/j.envpol.2010.03.022.
[14] M. Reymond, M. Descostes, C. Besançon, M. Leermakers, S. Billon, G. Cherfallot, M. Muguet, C. Beaucaire, V. Smolikova, P. Patrier, Assessment of 226Ra and U colloidal transport in a mining environment, Chemosphere 338 (2023) 139497, https://doi.org/10.1016/j.chemosphere.2023.139497.
[15] M. Leermakers, V. Phrommavanh, J. Drozdzak, Y. Gao, J. Nos, M. Descostes, DGT as a useful monitoring tool for radionuclides and trace metals in environments impacted by uranium mining: Case study of the Sagnes wetland in France, Chemosphere 155 (2016) 142–151, https://doi.org/10.1016/j.chemosphere.2016.03.138.
[16] M. Boudias, A. Gourgiotis, G. Montavon, C. Cazala, V. Pichon, N. Delaunay, 226Ra and 137Cs determination by inductively coupled plasma mass spectrometry: state of the art and perspectives including sample pretreatment and separation steps, J. Environ. Radioact. 244–245 (2022) 106812, https://doi.org/10.1016/j.jenvrad.2022.106812.
[17] D. Lariviere, V.F. Taylor, R.D. Evans, R.J. Cornett, Radionuclide determination in environmental samples by inductively coupled plasma mass spectrometry, Spectrochim. Acta Part B, At. Spectrosc. 61 (2006) 877–904, https://doi.org/10.1016/j.sab.2006.07.004.
[18] G. Xiao, Y. Liu, R.L. Jones, Determination of 226Ra in urine using triple quadrupole inductively coupled plasma mass spectrometry, Radiat. Prot. Dosimetry 191 (2020) 391–399, https://doi.org/10.1093/rpd/ncaa180.
[19] F.M. Wærsted, K.A. Jensen, E. Reinoso-Maset, L. Skipperud, High Throughput, Direct Determination of ^{226} Ra in Water and Digested Geological Samples, Anal. Chem. 90 (2018) 12246–12252, https://doi.org/10.1021/acs.analchem.8b03494.
[20] H. Ben Yaala, R. Fniter, D. Foucher, O. Clarisse, Direct analysis of radium-226 in sediment by ICP-MS: an analytical challenge? J. Anal. at. Spectrom. 34 (2019) 1597–1605, https://doi.org/10.1039/C9JA00156E.
[21] V.N. Epov, D. Lariviere, R.D. Evans, C. Li, R.J. Cornett, Direct determination of 226Ra in environmental matrices using collision cell inductively coupled plasma mass-spectrometry, J. Radioanal. Nucl. Chem. 256 (2003) 53–60, https://doi.org/10.1023/A:1023343824444.
[22] T. Zhang, D. Bain, R. Hammack, R.D. Vidic, Analysis of Radium-226 in High Salinity Wastewater from Unconventional Gas Extraction by Inductively Coupled Plasma-Mass Spectrometry, Environ. Sci. Technol. 49 (2015) 2969–2976, https://doi.org/10.1021/es504656q.
[23] L.H. Vieira, W. Geibert, I. Stimac, D. Koehler, M.M. Rutgers van der Loeff, The analysis of 226Ra in 1-liter seawater by isotope dilution via single-collector sector-field ICP-MS, Limnol. Oceanogr. Methods 19 (2021) 356–367, https://doi.org/10.1002/lom3.10428.
[24] F. Chabaux, D.B. Othman, J.L. Birck, A new Ra·Ba chromatographic separation and its application to Ra mass-spectrometric measurement in volcanic rocks, Chem. Geol. 114 (1994) 191–197, https://doi.org/10.1016/0009-2541(94)90052-3.
[25] C. Dalencourt, M.N. Chabane, J.-C. Tremblay-Cantin, D. Larivière, A rapid sequential chromatographic separation of U- and Th-decay series radionuclides in water samples, Talanta 207 (2020) 120282, https://doi.org/10.1016/j.talanta.2019.120282.
[26] M. Verlinde, J. Gorny, G. Montavon, S. Khalfallah, B. Boulet, C. Augeray, D. Larivière, C. Dalencourt, A. Gourgiotis, A new rapid protocol for 226Ra separation and preconcentration in natural water samples using molecular recognition technology for ICP-MS analysis, J. Environ. Radioact. 202 (2019) 1–7, https://doi.org/10.1016/j.jenvrad.2019.02.003.
[27] M. Roulier, P.A. Baya, S. Roberge, D. Larivière, Comparison of radium-226 separation methods based on chromatographic and extraction resins for its determination by ICP-MS in drinking waters, J. Mass Spectrom. 59 (2024) e5005.
[28] W. Davison, G.W. Grime, J.A.W. Morgan, K. Clarke, Distribution of dissolved iron in sediment pore waters at submillimetre resolution, Nature 352 (1991) 323–325, https://doi.org/10.1038/352323a0.
[29] R.J.G. Mortimer, M.D. Krom, P.O.J. Hall, S. Hulth, H. Ståhl, Use of gel probes for the determination of high resolution solute distributions in marine and estuarine pore waters, Mar. Chem. 63 (1998) 119–129, https://doi.org/10.1016/S0304-4203(98)00055-3.
[30] H. Dočekalová, O. Clarisse, S. Salomon, M. Wartel, Use of constrained DET probe for a high-resolution determination of metals and anions distribution in the sediment pore water, Talanta 57 (2002) 145–155, https://doi.org/10.1016/S0039-9140(01)00679-8.
[31] Y. Gao, M. Leermakers, C. Gabelle, P. Divis, G. Billon, B. Ouddane, J.-C. Fischer, M. Wartel, W. Baeyens, High-resolution profiles of trace metals in the pore waters of riverine sediment assessed by DET and DGT, Sci. Total Environ. 362 (2006) 266–277, https://doi.org/10.1016/j.scitotenv.2005.11.023.
[32] J. Huang, H. Franklin, P.R. Teasdale, M.A. Burford, N.R. Kankanamge, W. W. Bennett, D.T. Welsh, Comparison of DET, DGT and conventional porewater extractions for determining nutrient profiles and cycling in stream sediments, Environ. Sci. Process. Impacts 21 (2019) 2128–2140, https://doi.org/10.1039/C9EM00312F.
[33] M. Leermakers, Y. Gao, C. Gabelle, S. Lojen, B. Ouddane, M. Wartel, W. Baeyens, Determination of High Resolution Pore Water Profiles of Trace Metals in Sediments of the Rupel River (Belgium) using Det (Diffusive Equilibrium in Thin Films) and

DGT (Diffusive Gradients in Thin Films) Techniques, Water. Air. Soil Pollut. 166 (2005) 265–286, https://doi.org/10.1007/s11270-005-6671-7.
[34] M. Arsic, P.R. Teasdale, D.T. Welsh, S.G. Johnston, E.D. Burton, K. Hockmann, W. W. Bennett, Diffusive Gradients in Thin Films Reveals Differences in Antimony and Arsenic Mobility in a Contaminated Wetland Sediment during an Oxic-Anoxic Transition, Environ. Sci. Technol. 52 (2018) 1118–1127, https://doi.org/10.1021/acs.est.7b03882.
[35] A. Martin, Y. Hassan-Loni, A. Fichtner, O. Péron, K. David, P. Chardon, S. Larrue, A. Gourgiotis, S. Sachs, T. Arnold, B. Grambow, T. Stumpf, G. Montavon, An integrated approach combining soil profile, records and tree ring analysis to identify the origin of environmental contamination in a former uranium mine (Rophin, France), Sci. Total Environ. 747 (2020) 141295, https://doi.org/10.1016/j.scitotenv.2020.141295.
[36] A. Martin, G. Montavon, C. Landesman, A combined DGT - DET approach for an in situ investigation of uranium resupply from large soil profiles in a wetland impacted by former mining activities, Chemosphere 279 (2021) 130526, https://doi.org/10.1016/j.chemosphere.2021.130526.
[37] S. Grangeon, C. Roux, C. Lerouge, P. Chardon, R. Beuzeval, G. Montavon, F. Claret, T. Grangeon, Geochemical and mineralogical characterization of streams and wetlands downstream a former uranium mine (Rophin, France), Appl. Geochem. 150 (2023) 105586, https://doi.org/10.1016/j.apgeochem.2023.105586.
[38] T. Geng, O. Peron, A. Mangeret, L. Darricaut, M. Le Coz, K. David, C. Debayle, P. Blanchart, G. Montavon, A. Gourgiotis, Combining isotopic tracers and 238U-series disequilibrium to identify the origin of radioactive materials and their transport processes downstream of a former U mine site, Submitt. J Hazard Mater (n.d.).
[39] D.J. Condon, N. McLean, S.R. Noble, S.A. Bowring, Isotopic composition (238U/235U) of some commonly used uranium reference materials, Geochim. Cosmochim. Acta 74 (2010) 7127–7143, https://doi.org/10.1016/j.gca.2010.09.019.
[40] S. Richter, A. Alonso-Munoz, R. Eykens, U. Jacobsson, H. Kuehn, A. Verbruggen, Y. Aregbe, R. Wellum, E. Keegan, The isotopic composition of natural uranium samples—Measurements using the new n(233U)/n(236U) double spike IRMM-3636, Int. J. Mass Spectrom. 269 (2008) 145–148, https://doi.org/10.1016/j.ijms.2007.09.012.
[41] M. Boudias, S. Korchi, A. Gourgiotis, A. Combès, C. Cazala, V. Pichon, N. Delaunay, Screening of synthesis conditions for the development of a radium ion-imprinted polymer using the dummy template imprinting approach, Chem. Eng. J. 450 (2022) 138395, https://doi.org/10.1016/j.cej.2022.138395.
[42] C.N. Maréchal, P. Télouk, F. Albarède, Precise analysis of copper and zinc isotopic compositions by plasma-source mass spectrometry, Chem. Geol. 156 (1999) 251–273, https://doi.org/10.1016/S0009-2541(98)00191-0.
[43] W.A. Russell, D.A. Papanastassiou, T.A. Tombrello, Ca isotope fractionation on the Earth and other solar system materials, Geochim. Cosmochim. Acta 42 (1978) 1075–1090, https://doi.org/10.1016/0016-7037(78)90105-9.
[44] D.R. Lide, CRC Handbook of Chemistry and Physics, 85th Edition, CRC Press, 2004.
[45] M. Ohata, T. Ichinose, N. Furuta, A. Shinohara, M. Chiba, Isotope Dilution Analysis of Se in Human Blood Serum by Using High-Power Nitrogen Microwave-Induced Plasma Mass Spectrometry Coupled with a Hydride Generation Technique, Anal. Chem. 70 (1998) 2726–2730, https://doi.org/10.1021/ac971350f.
[46] J. Fietzke, V. Liebetrau, D. Günther, K. Gürs, K. Hametner, K. Zumholz, T. H. Hansteen, A. Eisenhauer, An alternative data acquisition and evaluation strategy for improved isotope ratio precision using LA-MC-ICP-MS applied to stable and radiogenic strontium isotopes in carbonates, J. Anal. at. Spectrom. 23 (2008) 955–961, https://doi.org/10.1039/B717706B.
[47] V.N. Epov, S. Berail, M. Jimenez-Moreno, V. Perrot, C. Pecheyran, D. Amouroux, O. F.X. Donard, Approach to Measure Isotopic Ratios in Species Using Multicollector-ICPMS Coupled with Chromatography, Anal. Chem. 82 (2010) 5652–5662, https://doi.org/10.1021/ac100648f.